

This item is the archived peer-reviewed author-version of:

Vulnerability assessment of atmospheric storage tanks to floods based on logistic regression

Reference:

Yang Yunfeng, Chen Guohua, Reniers Genserik.- Vulnerability assessment of atmospheric storage tanks to floods based on logistic regression
Reliability engineering and system safety - ISSN 0951-8320 - 196(2020), 106721
Full text (Publisher's DOI): <https://doi.org/10.1016/J.RESS.2019.106721>
To cite this reference: <https://hdl.handle.net/10067/1660950151162165141>

Highlights

1. Fragility models that can be widely used are proposed using logistic regression.
2. Effects of key parameters on vulnerability are analyzed using fragility curves.
3. Fragility magic cubes are first proposed to obtain the critical damage conditions.
4. Mitigation measures are proposed based on the results of vulnerability assessment.

Vulnerability assessment of atmospheric storage tanks to floods based on logistic regression

Yunfeng Yang^{a, b}, Guohua Chen^{a, *}, Genserik Reniers^{b, c, d}

^a *Institute of Safety Science and Engineering, South China University of Technology, Guangzhou 510640, People's Republic of China*

^b *CEDON, KU Leuven, 1000 Brussels, Belgium*

^c *Faculty of Technology, Policy and Management, Safety and Security Science Group (S3G), TU Delft, 2628 BX Delft, The Netherlands*

^d *Faculty of Applied Economics, Antwerp Research Group on Safety and Security (ARGoSS), University of Antwerp, 2000 Antwerp, Belgium*

ABSTRACT

Atmospheric storage tanks damaged by floods may lead to severe Natech accident scenarios, and the vulnerability assessment of process equipment suffered by natural events is a crucial point in Natech risk analysis. In the present study, limit state equations for failure modes of displacement and buckling are introduced based on load-resistance relationships. The parameterized fragility models that can be used in a wide variety of atmospheric unanchored storage tanks and floods have been developed based on logistic regression (LR), and moreover, the models are assessed and validated by receiver operating characteristic (ROC) curves and available accident data in the literatures. The effects of flood inundation height, velocity, liquid height and tank size on the vulnerability of different failure modes are analyzed using fragility curves. Furthermore, fragility magic cubes are first proposed to obtain the critical disaster conditions and critical filling levels in different cases. Finally, corresponding mitigation measures in different stages such as site selection, design, and operation are proposed based on the results of vulnerability assessment.

Keywords: flood disaster; vulnerability; fragility magic cubes; fragility curves; logistic regression

1. Introduction

The damage of process equipment triggered by natural disasters can result in serious consequences such as loss of containments, fires, and explosions, which are called as Natech events [1]. Floods and lightning are the most frequent natural disasters that trigger Natech events [2], and atmospheric storage tanks are the most vulnerable equipment suffered by floods [3]. Numerous severe accidents highlight the risk associated with floods impacting chemical facilities. For example, the liquid chlorine tanks were lifted by the flood occurred in the Czech Republic in the summer of 2002, resulting in leakage of 80 tons of liquid chlorine and 10 tons of chlorine gas [3]. Another example is the oil tanks damaged by the floods accompanied by Hurricane Katrina in 2005, resulting in the release of over 8 million gallons of oil and soil pollution in the affect area [4]. Therefore, it is of great significance to assess the risks of Natech events triggered by flood disasters and take some measures to mitigate those risks.

The key issue of Natech events quantitative risk assessment (QRA) is to develop the equipment vulnerability assessment models that can be used to assess the equipment damage probability based on the intensity parameters of natural disasters [5,6]. Most of the studies in the field of Natech risk assessment have focused on the risk assessment of process equipment to earthquakes [7,8,9,10] and lightning [11,12,13,14]. However, there are few studies on Natech events triggered by floods due to lack of historical data on detailed flood and equipment parameters, and these research mainly relied on the numerical techniques to obtain the failure probability. Landucci et al. developed the mechanical buckling failure models for atmospheric vertical storage tanks [15] and horizontal cylindrical vessels [16], and proposed the simplified correlations to calculate the failure probability of storage tanks based on the intensity parameters of floods. Furthermore, Antonioni et al. proposed a specific QRA methodology to assess the risk of Natech scenarios triggered by floods based on the above models and simplified correlations [17]. Similarly, Basco and Salzano developed the vulnerability functions to assess the impact of tsunami wave and debris on tanks [18]. Nevertheless, the models presented above are only for buckling failure, in fact, there is more than one failure mode of storage tanks suffered by floods. Khakzad and Gelder developed fragility models and curves for different failure modes such as floatation, buckling, and sliding based on LR [19] while Bayesian networks were

introduced to assess the system failure probability of atmospheric storage tanks to floods [4]. However, the fragility models are only applicable for a specific storage tank and flood, and those models should be redeveloped when evaluating other tanks or floods. Kameshwar and Padgett developed parameterized fragility models for the most common failure modes (floatation and buckling) of above ground storage tanks subjected to storm surge based on a dual layer metamodel, in addition, fragility curves varying with surge height are developed based on the above models [20]. But the fragility curves cannot reflect the effect of other parameters related to vulnerability such as liquid height and flood velocity.

This study seeks to analyze the failure modes of atmospheric unanchored storage tanks suffered by floods, and develop parameterized fragility models that can be used in a wide range of atmospheric unanchored storage tanks subject to flood with different intensities. Furthermore, this is the first study to propose the definition of fragility magic cubes to obtain the critical disaster conditions and critical filling levels in different cases. Finally, the results are helpful to risk assessment of the storage tanks to the floods, and can also provide guidance for the mitigation of tank failure subject to floods.

2. Methodology

2.1 Failure modes and limit state equations

Analyzing 272 Natech accidents triggered by floods from 1960 to 2007, Cozzani et al. found that the displacement of tanks due to sliding caused by water drag force or floatation caused by water buoyancy is the most common failure mode [3]. Additionally, buckling of tank walls due to hydrostatic and dynamic pressure is also identified as a potential failure mode in the literature [3,4,5,15,18,19,20,21]. Although debris accompanying with floods could also lead to the rupture of tank walls [19], this paper only studies the failure modes caused by floods directly, i.e., displacement and buckling. In this regard, limit state equations (LSEs) with respect to the above failure modes have been introduced based on a comparison between flood loads and the equipment resistance [4,15,18,19,20].

2.1.1 Displacement

Both the sliding and floatation failure could lead to the tanks drift from their original positions and result in the connection failure. Therefore, sliding and floatation can be considered as the same

failure mode: displacement.

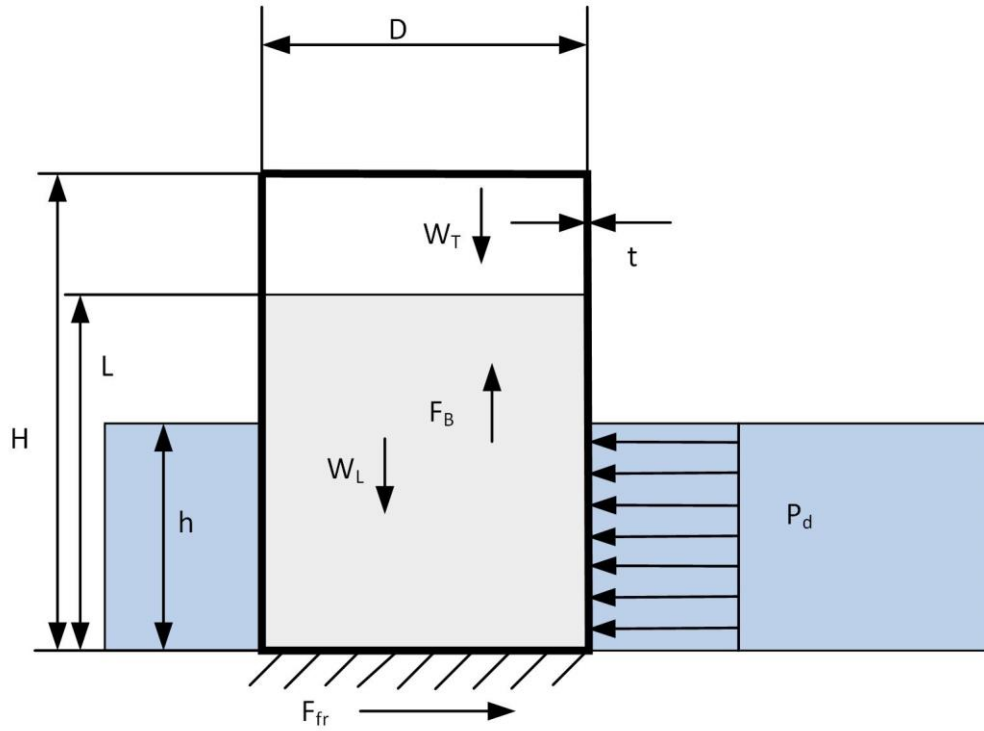


Fig.1 Schematic of the load-resistance forces considered for tank displacement (modified after the references [4,9]).

Fig.1 shows the forces acting on unanchored atmospheric storage tanks impacted by a flood wave considered for displacement failure. As shown in Fig.1, D , H , and t are the diameter, height, and thickness of tank. The height of the stored liquid and the flood inundation have been denoted, respectively, by L and h . Floatation failure is mainly due to the fact that the buoyancy of flood F_B in vertical direction is greater than the sum of the tank wall gravity W_T and the stored liquid gravity W_L . Although the specifications for the anchorage of storage tanks have been given in the current standards [21], most of the storage tanks in chemical plants are still unanchored tanks [22]. Therefore, the current work only considers the unanchored storage tanks for the sake of simplification.

The buoyancy of vertical direction can lead to the floating of storage tanks, and thus the limit state equation (LSE) for floatation failure, $LSE_{Floatation}$, can be expressed in Eqs. (1)-(4):

$$LSE_{Floatation} = F_B - W_T - W_L = -F_N \quad (1)$$

$$F_B = \rho_w g \frac{\pi D^2}{4} h \quad (2)$$

$$W_T = \rho_s g \left(\pi D H + 2 \frac{\pi D^2}{4} \right) t \quad (3)$$

$$W_L = \rho_l g \frac{\pi D^2}{4} L \quad (4)$$

where F_N is defined as the normal force exerted on the bottom of the tank from ground when the buoyancy is less than the gravity of tank wall and stored liquid, otherwise F_N only represents the difference value between gravity and buoyancy; ρ_w , ρ_s , and ρ_l are the densities (kg/m³) of the flood water, tank wall (usually steel), and stored liquid, respectively; $g= 9.81(\text{m/s}^2)$ is gravitational acceleration. As shown in Eq. (1), floatation failure will occur if $LSE_{\text{floatation}} > 0$.

As shown in Fig.1, if the horizontal hydrodynamic force of flood F_d is greater than the friction force F_{fr} between the tank and ground, the rigid sliding will occur, and the LSE for sliding failure LSE_{sliding} can be expressed using Eq. (5), where $LSE_{\text{sliding}} > 0$ indicates the sliding failure of the tank. The hydrodynamic force F_d can be obtained using the product of the hydrodynamic pressure P_d and the vertical wet section area of the tank, $D \times h$, as can be seen in Eqs. (6)-(7), where C_d is the drag coefficient ($C_d = 1.2$ for round piles); V is the average velocity of the flood (m/s). The friction force F_{fr} can be calculated as the product of the friction coefficient C_f and the normal force F_N under the situation that the tank is not floated (i.e., $F_N \geq 0$), as shown in Eq. (8).

$$LSE_{\text{sliding}} = F_d - F_{fr} \quad (5)$$

$$P_d = \frac{1}{2} C_d \rho_w V^2 \quad (6)$$

$$F_d = P_d D h \quad (7)$$

$$F_{fr} = C_f F_N \quad (8)$$

As can be seen from Eq. (1), if floatation failure occurred, the value of F_N is less than 0. Meanwhile, the value of F_{fr} is also assumed less than 0 based on Eq. (8) and the value of LSE_{sliding} is assumed greater than 0 based on Eq. (5) in this paper. Therefore, the LSE of displacement failure due to floatation and sliding can be expressed using Eq. (9), where $LSE_{\text{displacement}} > 0$ indicates the displacement failure of the tank.

$$LSE_{\text{displacement}} = F_d - F_{fr} \quad (9)$$

2.1.2 Buckling

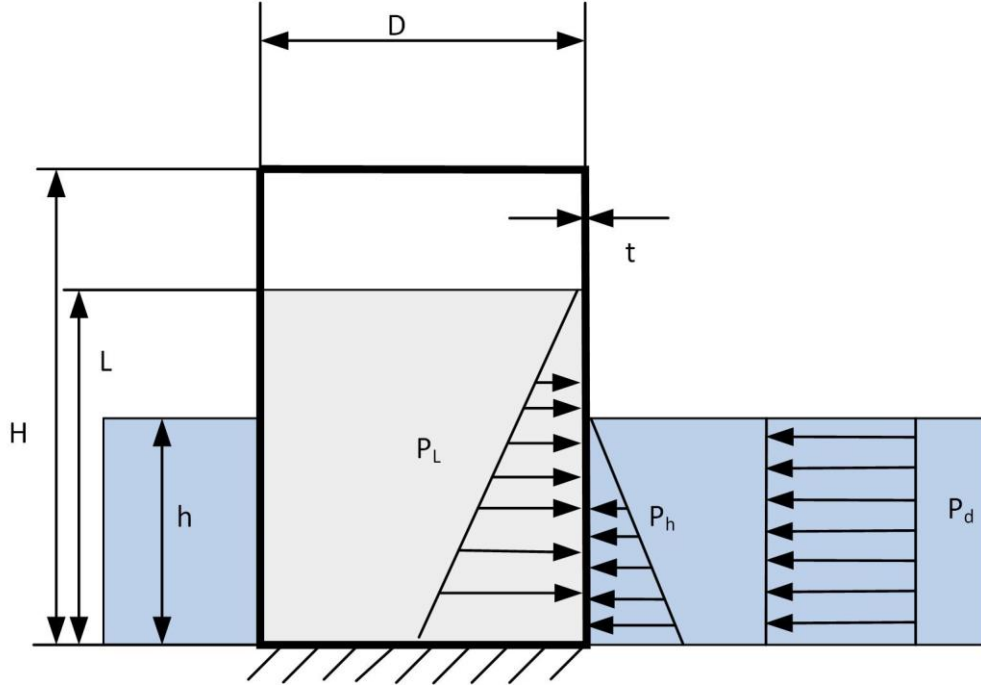


Fig.2 Schematic of the load-resistance forces considered for tank buckling (modified after the references [4,9]).

Excessive water pressure created by flood may result in the tank shell buckling, and the main resisting and loading radial pressure on the tank wall has been depicted in Fig.2. If the difference value between the radial pressure of loading and resisting is higher than a critical pressure, tank wall buckling occurs, and the LSE for buckling failure can be expressed by Eq. (10). As shown in Eq. (10), buckling failure will occur if $LSE_{Buckling} > 0$, where P_h is the static loading pressure due to the hydrostatic of the flood; P_L is the resisting pressure of tank related to the hydrostatic pressure of the stored liquid, as shown in Eq. (11). The values of hydrostatic pressure P_L and P_h which increase linearly with flood inundation height are calculated for the maximum values at the bottom of the tank.

$$LSE_{Buckling} = P_h + P_d - P_L - P_{cr} \quad (10)$$

$$P_L = \rho_l g L \quad (11)$$

$$P_h = \rho_w g h \quad (12)$$

P_{cr} is the critical pressure of the tank which depends on the tank geometry and the tank wall material, and it can be estimated using simplified relationships given in Eq. (13) for long cylinders

and in Eq. (14) for short cylinders, respectively [23], where E is the Elastic modulus of the tank material; ν is the Poisson's ratio.

$$P_{cr} = \frac{2E}{1-\nu^2} \left(\frac{t}{D}\right)^3 \quad (13)$$

$$P_{cr} = \frac{2.59Et^{2.5}}{HD^{1.5}} \quad (14)$$

2.2 Logistic regression

LR is a classification model in machine learning, which is widely used in the fields of medical fields and social sciences [24,25]. Furthermore, LR can also be used in engineering, especially to predict the failure probability of a given system [19,20,26]. Considering the tank can have only two possible states (failure or safety) when it suffered by flood, the binary logistic regression method was introduced to measure the relationship between the failure state and key independent variables (i.e., the flood inundation height, flood velocity, and liquid height) in the LSEs. Assuming $Y = 1$ if the tank is failure, otherwise $Y = 0$, a probability function $P(x) = P(Y = 1|X = x)$ can be used to predict the failure probability of the tank suffered by flood, where $P(x)$ represents the failure probability ranges between 0 and 1; X represents a set of independent variables. In order to show the relationship between the failure probability $P(x)$ and independent variables x , the linear logit function $\Phi(x)$ was introduced in Eq. (15), where $\beta_0, \beta_1 \dots \beta_n$ are the regression coefficients. It should be noted that the logit function is on an unrestricted scale, so a sigmoid function was used to transfer the output to a value between 0 and 1, as shown in Eq. (16).

$$\Phi(x) = \ln \frac{P(x)}{1-P(x)} = \beta_0 + \beta_1 x_1 + \beta_2 x_2 + \dots + \beta_n x_n \quad (15)$$

$$P(x) = \frac{1}{1 + e^{-\Phi(x)}} \quad (16)$$

The regression coefficients $\beta_0, \beta_1 \dots \beta_n$ are usually estimated using maximum likelihood estimation, and the likelihood function for m observations was developed as Eq. (17). To obtain fragility models, a set of 10000 random parameters are generated using a Monte Carlo simulation for each failure mode to span the entire ranges of applicable parameters described in Table 1. Furthermore, the LSEs for displacement and buckling are evaluated for all of the points, and step-wise LR is performed to obtain fragility models.

$$likelihood = \prod_{i=1}^m P(Y = y_i | X = x_i) = \prod_{i=1}^m P(x_i)^{y_i} [1 - P(x_i)]^{1-y_i} \quad (17)$$

As shown in Table 1, the diameters of tanks are assumed to follow a uniform distribution which range from 5 to 100 according to API 650 [21]; the tank heights correlated to the tank diameters can be obtained by the ratios of height to diameter [20]. It should be noted that the fire dike should higher than the design floor more than 1m and the foundation of the tank should be higher than 0.5m [27], thus the minimum flood inundation height is set to 0.5m.

Table 1 Parameters used for vulnerability assessment of storage tank.

Parameter	Distribution	Reference
Diameter of tank D (m)	Uniform (5, 100)	[21]
Height of tank H (m)	ϕH	-
Ratio of height to diameter $\phi=H/D$	$e^{0.25(1-2\ln D)} \leq e^{3.07-0.95\ln D}$	[20]
Minimum shell thickness t_{\min} (mm)	5 ($D < 15$); 6 ($15 \leq D < 36$); 8 ($36 \leq D \leq 60$); 10 ($D > 60$)	[21]
Shell thickness t (mm)	$t = \frac{4.9D(H-0.3)\rho_s}{S_d} + CA$	[21]
Corrosion allowance CA (mm)	3	[21]
Allowable stress for the design condition S_d (MPa)	260	[21]
Flood velocity V (m/s)	Uniform (0, 5)	[3]
Flood inundation height h (m)	Uniform (0.5, 5)	[3]
Flood water density ρ_w (kg/m ³)	1024	[4]
Tank shell density (steel) ρ_s (kg/m ³)	7900	[4]
Crude oil density ρ_l (kg/m ³)	850	[4]
Height of storage liquid L (m)	Uniform (0.1 H , 0.9 H)	Assumed

2.3 Parameterized models and model verification

2.3.1 Parameterized models

A Monte Carlo simulation is used to generate 10000 random values of LSE as Eqs. (9) and (10). In this regard, the positive values of LSE are considered as an indication of the tank displacement or buckling, $Y = 1$; whereas negative values are considered as the tank not failure, $Y = 0$. For each combination of parameters, the parameter distributions are listed in Table 1, and D, H, L, h, V are the random variable playing a key role in the LSE. Furthermore, influential parameter combinations of the logit function are determined by the form of LSE. The optimal values of $\beta_0, \beta_1 \cdots \beta_n$ are estimated using the maximum likelihood estimation analysis. For displacement failure, the logit

function of the trained LR model is shown in Eq. (18):

$$\begin{aligned} \Phi(D, H, L, V, h)_{\text{Displacement}} = & 0.03583D - 0.0005474H - 0.8264L \\ & -0.01384V + 0.5242h + 0.1545Dh + 0.3889Vh + 0.0003185D^2L \\ & -0.0003329D^2h - 0.0003928D^2 - 0.004784DH - 0.1293DL \\ & -0.0009968DV - 0.00161DVh - 0.145 \end{aligned} \quad (18)$$

In exactly the same way, the logit function of buckling can be expressed by Eq. (19):

$$\begin{aligned} \Phi(D, H, L, V, h)_{\text{Buckling}} = & 0.01419D + 0.04545H - 2.907L \\ & + 1.602V + 3.564h - 4.576 \end{aligned} \quad (19)$$

The failure probability of each failure mode can be calculated using Eq. (16) when the logit functions are determined. In the present study, we assumed that the failure of displacement and buckling are independent of each other, so the system failure probability of tank can be expressed by Eq. (20):

$$P = 1 - (1 - P_D)(1 - P_B) \quad (20)$$

where P_D is the probability of displacement, and P_B is the probability of buckling.

2.3.2 Model verification

In order to assess the performance of the parameterized models, ROC curve was introduced in the present study due to its both simplicity and practicality. A ROC curve is a graph showing the diagnostic ability of the binary classifier system as its discriminant threshold is varied. The ROC curve is developed by drawing the true positive rate (TPR) versus false positive rate (FPR) at various threshold settings. TPR defines the proportion of correct positive results upon the total number of positive samples during testing, FPR, on the other hand, defines the proportion of incorrect positive results upon the total number of positive samples during testing [28]. The results of ROC analysis of the LR have been displayed in Fig. 3, which is used to assess the LR's performance as a classifier. To this end, the dataset generated by a Monte Carlo simulation were compared with corresponding data computed by the LR. As can be seen from Fig.3, ROC curves for all the failure modes lie well above the line of no discrimination (LND), implying the high performance of the LR in predicting these failure modes. Besides, the accuracy of the BN in predicting the failure modes are $ACC_{\text{Displacement}} = 0.9988$, $ACC_{\text{Buckling}} = 0.9898$, respectively. This shows that the model can predict the failure modes of displacement and buckling well.

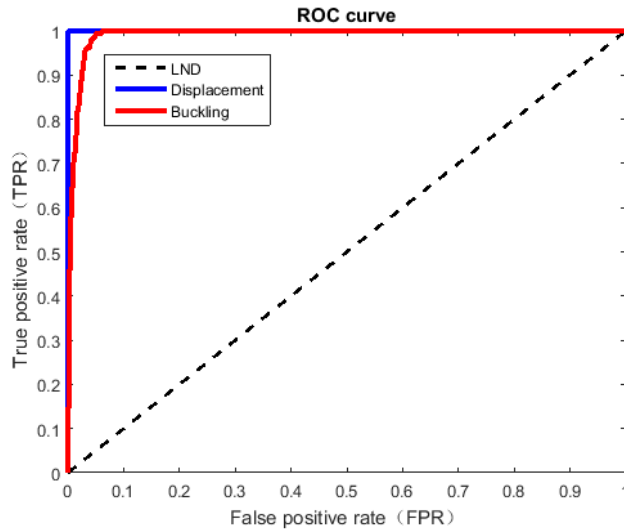


Fig.3 Performance assessment of the LR using ROC technique.

In order to further verify the accuracy of the model, the available literature data on past accidents has been introduced to compare with the results of the displacement failure. Due to the scarcity of detail historical data of buckling, the buckling failures obtained by reference [15] were compared with the results of the buckling failure. The results of verification indicate that the models can be used to calculate the failure probabilities of the tank subject to floods.

Table 2 The results of verification of available literature data on past accidents

Number	Failure modes	D(m)	H(m)	L(m)	H(m)	V(m/s)	P	References
1	Displacement	17.07	11.11	1.1	3.5	3	1	[29]
2	None	17.07	11.11	1.1	3.5	3	0.0039	[29]
3	Displacement	10.98	6.23	2.5	3.5	3	0.997	[29]
4	None	10.98	6.23	5.3	3.5	3	0.4072	[29]
5	Displacement	18.1	10.98	1.1	3.5	3	1	[29]
6	none	18.1	10.98	7	3.5	3	0	[29]
7	Buckling	36	9	0.9	1.2	2	0.77	[15]
8	Buckling	12	14.4	1.44	2.4	2	0.98	[15]

3. Results and discussions

In order to illustrate the applicability of the fragility models and assess the effects of parameters change on storage tank vulnerability, six unanchored atmospheric storage tanks with volumes range from 1000m^3 to $150,000\text{m}^3$ are selected as a case study, as shown in Table 3. Fragility curves are used to demonstrate the vulnerability variation of different failure modes with the parameters as follows: flood inundation height, flood velocity, storage liquid height and tank size. Moreover, fragility magic cubes are developed to obtain the failure states and critical filling levels under given flood events.

Table 3 The tank dimensions in the case study

Number	D(m)	H(m)	C(m ³)
T1	15	6	1000
T2	27	7.2	4000
T3	30	14	9000
T4	48	12.6	22000
T5	72	10.8	43000
T6	95	20	150000

3.1 Fragility curves

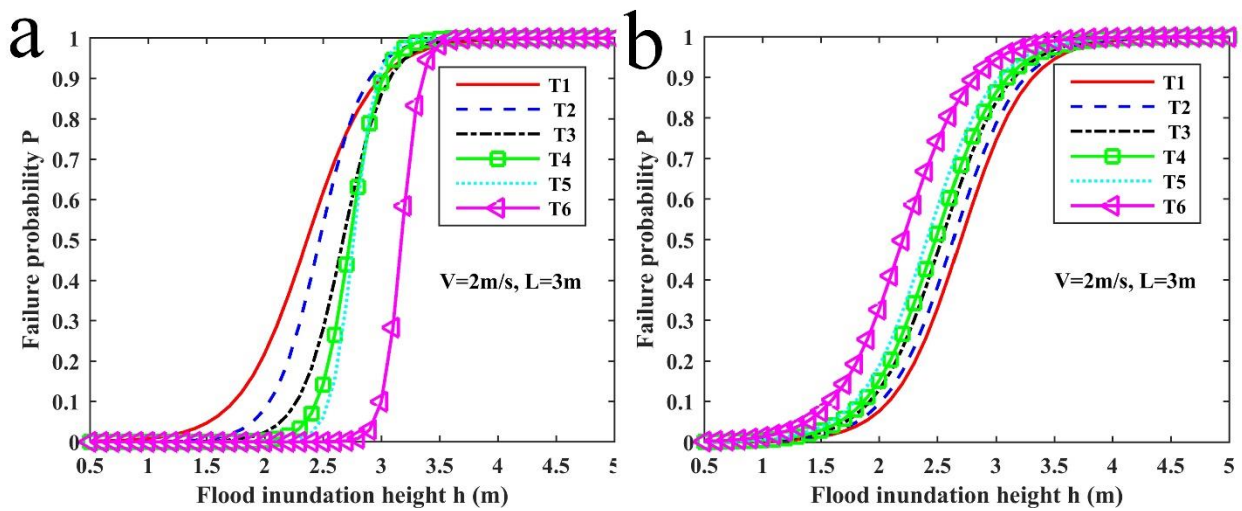


Fig.4 Fragility curves for tanks with different sizes: (a) displacement failure; (b) buckling failure.

The displacement and buckling fragility curves for different tanks are shown in Fig.4 (a) and (b) respectively, in addition, it should be noted that the liquid height and flood velocity are selected as 3m and 2m/s. It is apparent from this figure that small tanks are more prone to displacement failure than that of large tanks, due to the lower weight of tare and liquid stored in tanks; while large diameter tanks are more easily to occur buckling failure than that of small tanks, because of the low critical pressure, and the results are consistent with other research which found that high capacity vessels have high buckling probability [15]. Fig.5 shows the system fragility curves for different tanks, and from this graph we can see that the tank size has little effect on the probability of system failure.

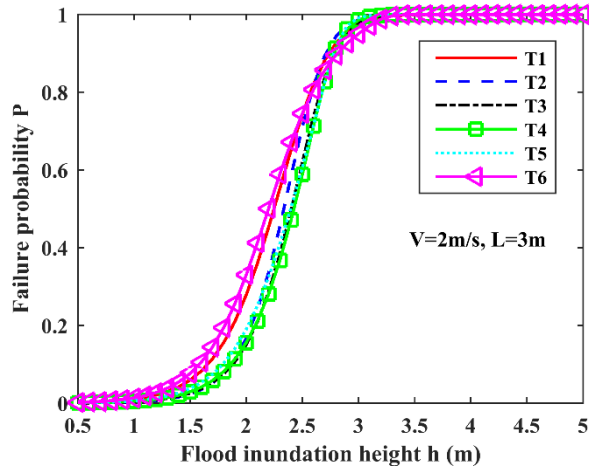


Fig.5 System fragility curves for tanks with different sizes

In order to assess the effects of different flood velocities on the vulnerability of displacement and buckling, T4 tank was selected as an example assuming that the liquid height is 3m and flood velocities range from 0m/s to 5m/s, and the results are shown in Fig.6. From this figure, it can be seen that the influence of the flood velocity on the buckling failure is larger than that of the displacement, owing to the hydrodynamic pressure induced by flood flow has the greater impact on buckling failure than that of displacement.

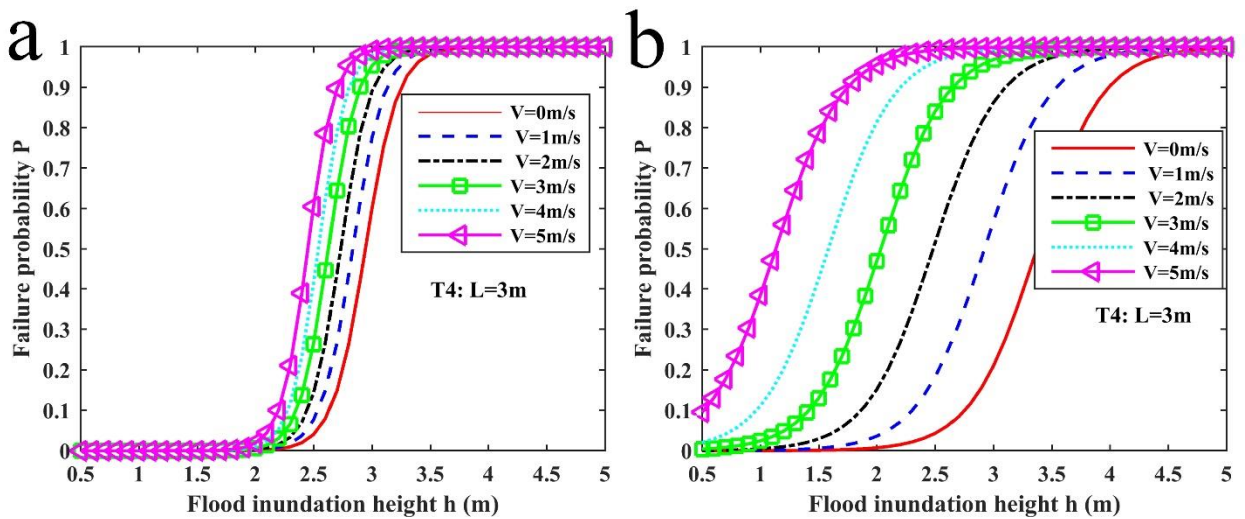


Fig.6 Fragility curves for T4 tank with different flood velocities: (a) displacement failure; (b) buckling failure.

Fig.7 (a) and (b) present the displacement and buckling fragility curves for T4 tank with liquid heights range from 2m to 7m, and the flood velocity is selected as 2m/s. As can be seen from Fig.7, the ranges of probability variation of displacement failure are greater than that of buckling failure

when the heights of stored liquid increase by 1m, and this indicates that the influence of liquid height on displacement failure is greater than that of buckling failure. Furthermore, the influence of flood inundation height on displacement failure is greater than buckling failure, due to the slopes of the displacement failure curves are greater than that of buckling failure curves.

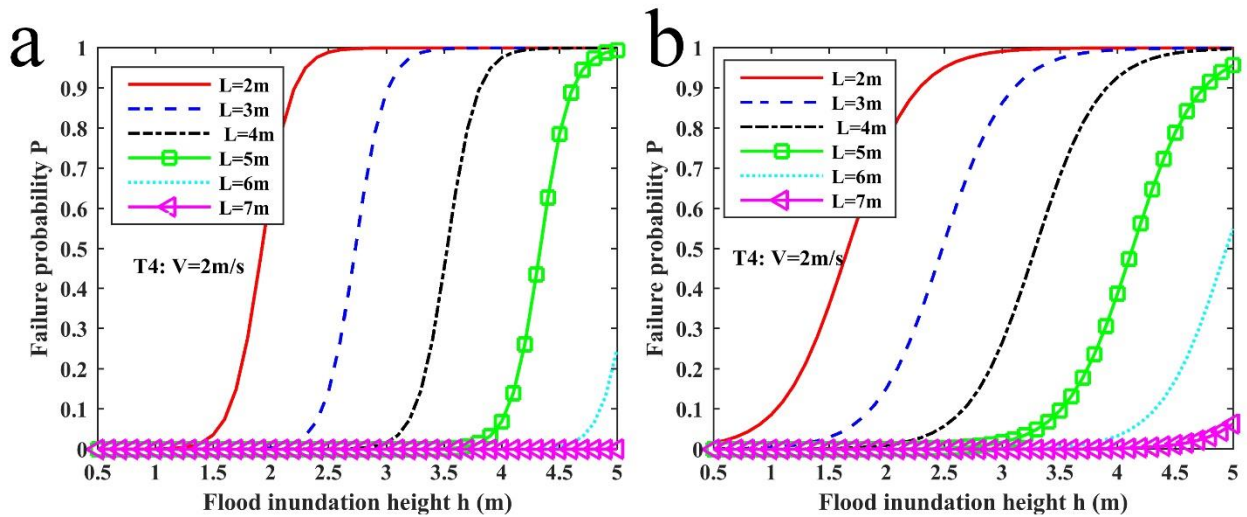


Fig.7 Fragility curves for T4 tank with different liquid heights: (a) displacement failure; (b) buckling failure.

In order to find out which failure mode is the dominate failure mode in different cases, Fig.8 (a) is selected as the reference case, and Fig.8 (b), (c) and (d) are used to explain the effects of flow velocity, stored liquid height and tank size on dominate failure modes respectively. From Fig.8 (a) we can see that the failure probabilities of buckling are larger than that of displacement when the flood inundation heights are less than 2.8m, while the failure probabilities of displacement are larger than that of buckling when flood inundation heights are greater than 2.8m. The results indicate that the buckling failure is the dominate failure mode at low flood inundation height assuming that flood velocity is 2m/s and liquid height is 3m. By comparing Fig.8 (a), (b) and (d) with (a), it could be concluded that the buckling failure may be the dominate failure mode with the increasing of the flood velocity or the volumes of tanks. Furthermore, the stored liquid height has relatively little impact on the dominate failure mode when comparing Fig.8 (a) and (c). Overall, these results indicate that the dominate failure mode depends on the combinations of different parameters, and the failure probability of the system is similar to that of the dominate failure mode.

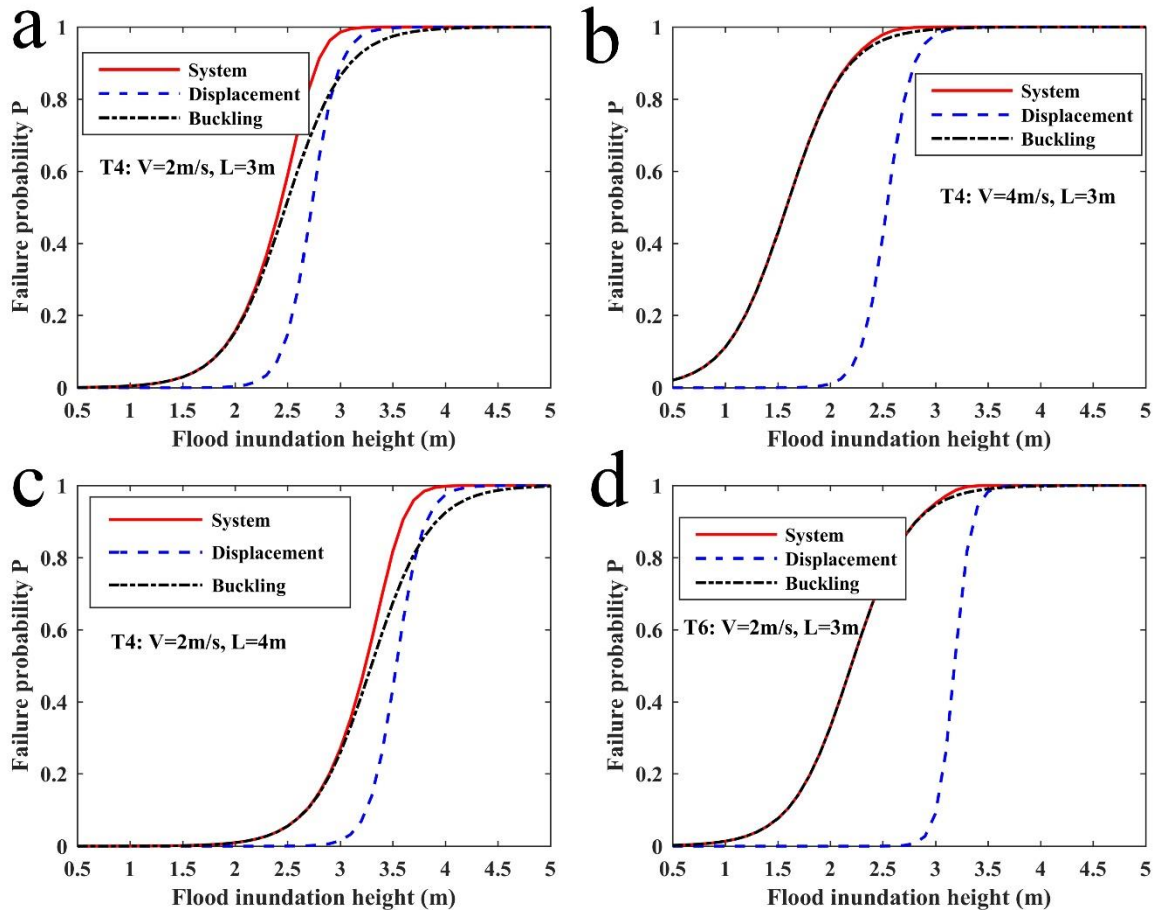


Fig.8 Fragility curves for the variations of dominant failure modes in different cases

3.2 Fragility magic cubes

From the above analysis, for a specific tank, the vulnerability is influenced by three key parameters: the height of stored liquid, the flood inundation height and velocity. In order to study the influence of different parameter combinations on the system vulnerability and assess the critical disaster conditions and critical filling levels in different cases, the fragility magic cubes were first developed as shown in Fig.9. The three key parameters are represented by three coordinate axes in the magic cubes, and system failure probabilities are expressed with different colors. From Fig.9 (a), we can obtain the failure probabilities and failure states under the most serious flood situation, such as the highest flood inundation depth and the maximum flood velocity. It could also be seen from Fig.9 (a) that if the storage height was greater than 8 meters, the tank would not be damaged by any flood disasters. Furthermore, the failure states under the lowest flood inundation height and the minimum flood velocity in different heights of stored liquid can also be obtained according to Fig.9 (b) which is the back of the fragility magic cube in Fig.9 (a). When the flood inundation height is

about 0.5m, the storage tanks seldom damaged by flood disasters only when the flood velocity is about more than 4m. Furthermore, if the stored liquid height is about more than 6m, the storage tank would not be damaged by any static flood disasters.

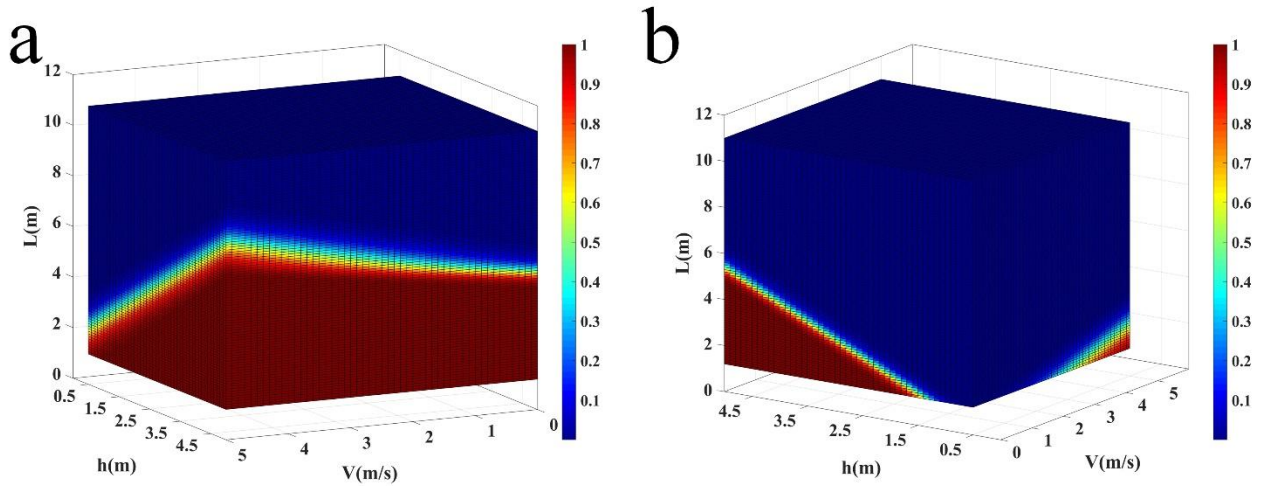


Fig.9 Fragility magic cubes of T4 tank in extreme conditions: (a) the most serious situation; (b) the least serious situation.

It is generally known that different areas suffered flood with different severities, and not all tank farms suffered the most extreme flood disasters. In order to study the vulnerability of storage tanks suffered by flood disasters with different intensities, the failure states and the critical filling levels under given flood events could be obtained by slicing the fragility magic cubes, as shown in Fig.10. Fig.10 presents the vulnerability of T4 suffered by the flood with the inundation is 2.5m and velocity is 2.5m/s. It could be concluded that the storage tank would not fail when suffered by the above mentioned flood as long as the height of storage liquid is more than 6m.

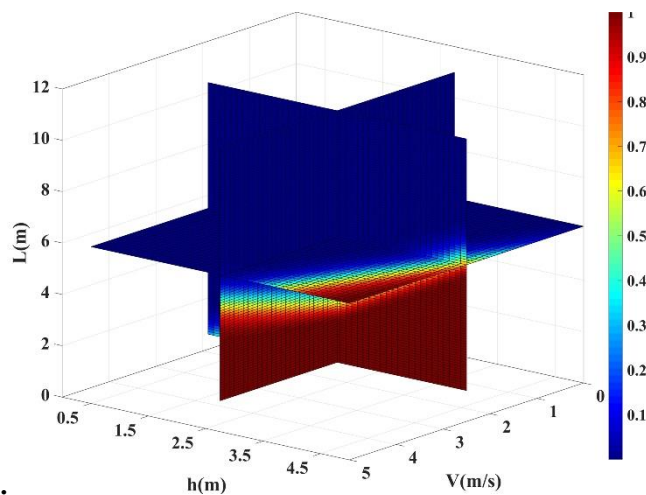


Fig.10 Slices of fragility magic cube of T4 tank in the concerned case.

3.3 Mitigation measures

In order to reduce accidents caused by the failure of tanks suffered by flood disasters, the targeted mitigation measures are put forward from the site selection, design and operation stages of tanks based on above analysis and other literatures. Firstly, in the case of meeting other standards of tank layouts, the location of the tank farm should be avoided in flood prone areas and arranged at a high terrain in the stage of site selection. Secondly, in the design stage, the flood inundation height could be effectively reduced by increasing the height of protective embankment and foundation of storage tank, in addition, the anchorage tank can effectively reduce the displacement failure [20] and the buckling failure can be effectively reduced by increasing the thickness of the tank wall [15]. Finally, during the operation stage, the height of stored liquid should be kept above the critical height before the flood, so that the tank cannot be damaged by the flood disaster.

4. Conclusions

The parameterized models of atmospheric tanks for displacement and buckling failure to flood are developed based on logistic regression, and the models are assessed and validated using ROC curves and historical accidents data. System failure probabilities of tanks are obtained based on the failure of displacement and buckling, assuming that the displacement and buckling failure are independent to each other. Six atmospheric storage tanks which cover a wide range of dimensions are selected for a case study to demonstrate the application of the fragility models.

In the case study, the effects of different parameters on the failure modes of displacement, buckling and system are analyzed using fragility curves. A small tank is more prone to displacement failure, while a larger tank is more prone to buckling failure, and the tank size has little effect on the probability of system failure. The influence of the flood velocity on the buckling failure is larger than that of the displacement, while the influence of stored liquid height and flood inundation height on displacement failure is greater than buckling failure. Furthermore, the dominate failure modes of different tank sizes are depend on the flood intensities and liquid filling levels. Fragility magic cubes are first developed to assess the critical disaster conditions and critical filling levels at the most and least serious situation respectively, and the failure states and the critical filling levels under given

flood events can be obtained by slicing the fragility magic cube.

The parameterized vulnerability models can effectively be applied to a wide variety of atmospheric unanchored storage tanks subject to floods with different intensities. The results are helpful to risk assessment of the storage tanks to the floods, and can also provide guidance for the prevention of tank failure subject to floods. Furthermore, this methodology can also be extended to pressure storage tanks and atmospheric anchored storage tanks.

Acknowledgements

This study was supported by the National Key R&D Program of China (2016YFC0801500), the National Natural Science Foundation of China (21576102), and China Scholarship (201806150064). We also appreciate those who assisted us with observations, the anonymous reviewers, and the editor for their constructive comments and suggestions.

References

- [1] Young S, Balluz L, Malilay J. Natural and technologic hazardous material releases during and after natural disasters: a review. *Sci Total Environ* 2004; 322(1-3): 3-20.
- [2] Krausmann E. Analysis of Natech risk reduction in EU Member States using a questionnaire survey. Report EUR 2010; 24661.
- [3] Cozzani V, Campedel M, Renni E, et al. Industrial accidents triggered by flood events: analysis of past accidents. *J Hazard Mater* 2010; 175(1-3): 501-509.
- [4] Khakzad Rostami N, van Gelder P. Vulnerability of industrial plants to flood-induced natechs: A Bayesian network approach. *Reliab Eng Syst Saf* 2018; 169: 403-411.
- [5] Antonioni G, Bonvicini S, Spadoni G, et al. Development of a framework for the risk assessment of Na-Tech accidental events. *Reliab Eng Syst Saf* 2009; 94(9): 1442-1450.
- [6] Salzano E, Agreda A G, Di Carluccio A, et al. Risk assessment and early warning systems for industrial facilities in seismic zones. *Reliab Eng Syst Saf* 2009; 94(10): 1577-1584.
- [7] Antonioni G, Spadoni G, Cozzani V. A methodology for the quantitative risk assessment of major accidents triggered by seismic events. *J Hazard Mater* 2007; 147(1-2):48-59.
- [8] Fabbrocino G, Iervolino I, Orlando F, et al. Quantitative risk analysis of oil storage facilities in seismic areas. *J Hazard Mater* 2005; 123(1-3):61-69.

- [9] Salzano E, Iervolino I, Fabbrocino G. Seismic risk of atmospheric storage tanks in the framework of quantitative risk analysis. *J Loss Prev Process Ind* 2003; 16(5):403-409.
- [10] Lanzano G, Salzano E, Magistris F S D, et al. Seismic vulnerability of natural gas pipelines. *Reliab Eng Syst Saf* 2013; 117(5):73-80.
- [11] Yang Y, Chen G, Chen P. The probability prediction method of domino effect triggered by lightning in chemical tank farm[J]. *Process Saf Environ Prot* 2018; 116:106-114.
- [12] Necci A, Antonioni G, Cozzani V, et al. A model for process equipment damage probability assessment due to lightning. *Reliab Eng Syst Saf* 2013; 115(7):91-99.
- [13] Necci A, Antonioni G, Cozzani V, et al. Assessment of lightning impact frequency for process equipment. *Reliab Eng Syst Saf* 2014; 130:95-105.
- [14] Necci A, Antonioni G, Bonvicini S, et al. Quantitative assessment of risk due to major accidents triggered by lightning. *Reliab Eng Syst Saf* 2016; 154:60-72.
- [15] Landucci G, Antonioni G, Tugnoli A, et al. Release of hazardous substances in flood events: Damage model for atmospheric storage tanks. *Reliab Eng Syst Saf* 2012; 106:200-216.
- [16] Landucci G, Necci A, Antonioni G, et al. Release of hazardous substances in flood events: Damage model for horizontal cylindrical vessels. *Reliab Eng Syst Saf* 2014; 132(132):125-145.
- [17] Antonioni G, Landucci G, Necci A, et al. Quantitative assessment of risk due to NaTech scenarios caused by floods. *Reliab Eng Syst Saf* 2015; 142:334-345.
- [18] Basco A, Salzano E. The vulnerability of industrial equipment to tsunamis. *J Loss Prev Process Ind* 2017;50:301-307.
- [19] Khakzad N, Van Gelder P. Fragility assessment of chemical storage tanks subject to floods. *Process Saf Environ Prot* 2017; 111: 75-84.
- [20] Kameshwar S, Padgett J E. Storm surge fragility assessment of above ground storage tanks. *Struct Saf* 2018; 70:48-58.
- [21] API Standard 650. *Welded Tanks for Oil Storage*. American Petroleum Institute 2007; Washington. D.C.
- [22] Godoy L A. Performance of storage tanks in oil facilities damaged by Hurricanes Katrina and Rita. *J Perform Constr Fac* 2007; 21(6): 441-449.
- [23] Timoshenko S P, Gere J M, Prager W. *Theory of Elastic Stability*, Second Edition. *J Appl Mech* 1962; 29(1):220.
- [24] Boyd C R, Tolson M A, Copes W S. Evaluating trauma care: the TRISS method. Trauma Score and the Injury Severity Score. *J Trauma* 1987; 27(4): 370-378.
- [25] Freedman D A. *Statistical models: theory and practice*. Oxford: Cambridge university press; 2009.

- [26] Palei S K, Das S K. Logistic regression model for prediction of roof fall risks in bord and pillar workings in coal mines: An approach. Saf Sci 2009; 47(1): 88-96.
- [27] GB 50074. Code for design of oil depot. National Standard of People's Republic of China 2014; Beijing.
- [28] Fawcett T. An introduction to ROC analysis. Pattern recogn lett 2006; 27(8): 861-874.
- [29] Yozo G. Tsunami damage to oil storage tanks. The 14thWorld Conference on Earthquake Engineering 2008; Beijing.